AN IMPROVED CSA FOR ONE-STATIONARY BISAR SQUINT MODE

Zeng Dazhi, Wang Rui, Long Teng and Zeng Tao*

Department of Electrical Engineering, Beijing Institute of Technology, P. R. China, 10081

1. INTRODUCTION

Bistatic Synthetic Aperture Radar (BiSAR) has been the focus in the recent years. One-stationary BiSAR squint mode system is constructed by a stationary receiver and the moving transmitter with squint angle. The benefit of squint mode is that it can enlarge bistatic angle and doesn't increase the space variability of echo data. Existing algorithms for this kind of BiSAR mentioned in the paper [1] and [2] ignore the remaining cubic phase and the space variability of the equivalent range FM rate after range cell migration correction (RCMC). The methods in the paper [3] and [4] are fit for the general BiSAR construction, but it becomes low efficiency for serious space variability. The algorithm presented in this paper can be more effective to deal with the space variability of this kind of BiSAR.

This paper is organized as follows. The second section establishes signal model firstly and some restraints for the imaging algorithm are obtained by analysis. The improved chirp scaling (CS) algorithm is proposed and the method of nonlinear chirp scaling (NLCS) is introduced in the third section. In the fourth section, simulation results are shown to verify the feasibility and effectiveness of the algorithm proposed. In the fifth section, the conclusion is drawn.

2. SIGNAL CHARACTERISTIC ANALYSIS

The geometry structure of one-stationary BiSAR is shown in Fig. 1.

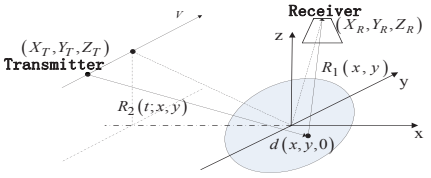

Fig. 1. One-stationary BiSAR geometry

We suppose the transmitted signal is $s(\tau;x,y)=\omega_R(\tau)\exp\left(-j\pi K_r\tau^2+j2\pi f_0\tau\right)$, where $\omega_R(\tau)$ is the envelop， K_r is the FM rate and f_0 is the carrier frequency. Then the echo from the target $d(x,y,0)$ can be written as

* Corresponding author

$$s(\tau,t;x,y)=\omega_R(\tau-\tau_d)\,\omega_A(t-t_d(y))\times\exp\left(-j\pi K_r(\tau-\tau_d(t;x,y))^2\right)\times\exp\left(-j2\pi f_0\tau_d(t;x,y)\right) \tag{1}$$

where $\omega_A(\bullet)$ is the azimuth beam envelope, $t_d(y)=(y-Y_T)/V$ represents the position information of the target in the azimuth, $\tau_d(t;x,y)=R(t;x,y)/c$ is the target delay and $R(t;x,y)=R_R(x,y)+R_T(t;x,y)$ is the bistatic range sum. By using the principle of stationary phase, the eq. (1) can be expressed in the range-Doppler domain as

$$\begin{aligned}S_1(\tau,f_t;x,y)=&C_0\omega_R\left(K_r'(R_{20},f_t)(\tau-\tau_d(f_t))\right)\omega_A\left(-\sqrt{1-D_0^2}R_{T0}/D_0\right)\\&\times\exp\left\{-j2\pi f_t t_d(y)\right\}\exp\left\{-j\frac{2\pi}{\lambda}\left(R_R(x,y)+R_{T0}D_0\right)\right\}\exp\left\{-j\pi K_e(R_{T0},f_t)(\tau-\tau_d(f_t))^2\right\}\end{aligned} \tag{2}$$

where $\tau_d(f_t)=(R_0+R_{T0}C_s)/c$ is the delay related to Doppler frequency, and $R_{T0}=\sqrt{(x-X_T)^2+Z_T^2}$ is the minimal range from the target to the moving platform.

$$R_0=R_R(x,y)+R_{T0}=\sqrt{\left(\sqrt{R_{T0}^2-Z_T^2}+X_T-X_R\right)^2+(y-Y_R)^2+Z_R^2}+R_{T0} \tag{3}$$

$$D_0=\sqrt{1-(cf_t/(f_0V))^2},C_s=1/D_0-1 \tag{4}$$

$$K_e(f_t,R_{T0})=1/\left(1/K_r+cR_{T0}f_t^2/\left(f_0^3V^2D_0^3\right)\right) \tag{5}$$

$R_0(R_{T0},y)$ is the minimal bistatic range sum. D_0 is the migration factor. $K_e(f_t,R_{T0})$ is the equivalent range FM rate. Through eq. (3)-(5), it can be found that $K_e(f_t,R_{T0})$ and the modulation in the azimuth direction vary with R_0 and y. The constraints caused by the equivalent range FM rate and modulation for imaging algorithm can be summarized as the following two aspects.

(1) In the squint mode, the variation of $K_e(f_t,R_{T0})$ with R_0 needs to be compensated.

(2) Echo data needs to be divided into several separate parts in the azimuth direction to solve the space variability problems. One reason is that $K_e(f_t,R_{T0})$ is variational with y, but it only exists in the Doppler domain without the information of y. It means that the variation of $K_e(f_t,R_{T0})$ with y can't be compensated. The other reason is that the modulation in the azimuth direction is also variational with y.

3. IMPROVED CSA

After 2-D FFT, the phase of echo signal can be approximately expressed as follow:

$$\Theta(f_\tau,f_t;x,y)=\Theta_0(f_t;x,y)+\Theta_1(f_t;x,y)f_\tau+\Theta_2(f_t;x,y)f_\tau^2+\Theta_3(f_t;x,y)f_\tau^3 \tag{6}$$

Firstly $\Theta(f_\tau,f_t;x,y)$ is multiplied by the cubic filter factor $\Theta_{CPF}=Y(f_t)f_\tau^3$, and then after range IFFT, the phase of the signal can be written as

$$\Theta_1=\Theta_0-\pi K_e(\tau-\tau_d(f_t))^2-Y_mK_e^3(\tau-\tau_d(f_t))^3 \tag{7}$$

where Θ_0 relates to the modulation in the azimuth and $Y_m=Y+\Theta_3(f_t;x,y)$. Then NLCS is introduced as

$$\Theta_{NCS}=-\pi q_2(\tau-\tau_{d\_ref})^2-j\pi q_3(\tau-\tau_{d\_ref})^3 \tag{8}$$

where $\tau_{d\_ref} = \left(R_{0\_ref} + R_{T0\_ref} C_s\right)/c$. R_{0_ref} and R_{T0_ref} are generally chosen in the center of the divided scene. After NLCS, we expand Θ_1 at $\tau = \tau_0 = \left(R_0 + R_{T0\_ref} C_s\right)/c$ to its Taylor series, and based on the following assumption: (1) linear phase is constantly zero, (2) quadratic phase factor has nothing to do with R_0, (3) cubic phase is constantly zeros, q_2, q_3 and Y_m can be deduced out. In the derivation, it can be found that q_3 has different expressions under the condition of (1) and (2), and can be respectively expressed as $2/3 \times k_s \xi C_s c / \left(1 - \left(C_s \xi\right)^2\right)$ and $-1/3 \times c k_s / \left(1 + \xi C_s\right)$. However, q_3 can be selected within the tolerable errors as

$$q_3 = a \bullet \left(-\frac{1}{3} \frac{k_s \bullet c}{1 + \xi C_s} \right) + b \bullet \left(\frac{2}{3} \frac{k_s \xi C_s c}{1 - \left(\xi C_s\right)^2} \right) \tag{9}$$

where $a + b = 1 \; and \; a, b \in [0,1]$. In the derivation, the approximations are used in $K_e \approx K_{e\_ref} + k_s \left(R_0 - R_{0\_ref}\right)$ and $R_{T0} - R_{T0\_ref} \approx \xi \bullet \left(R_0 - R_{0\_ref}\right)$, where $q_2 = K_{e\_ref} C_s \xi$ and $Y_m = -\pi q_3 / {K_{e\_ref}}^3$. After these reasonable processes, the matching function of range and azimuth can be respectively written as

$$\Theta_{range}\left(f_\tau, f_t; x, y\right) = \exp\left(-j\pi f_\tau^2 / \left(K_{e\_ref} + q_2\right) + j2\pi f_\tau R_{T0\_ref} C_s / c\right) \tag{10}$$

$$\Theta_{Azimuth}\left(f_t; x, y\right) = \exp\left(j2\pi R_{T0}\left(R_0, y = y_{ref}\right) \bullet \left(D_0 - 1\right)/\lambda\right) \tag{11}$$

where $R_{T0}\left(R_0, y\right)$ can be obtained by eq. (3). y_{ref} is generally chosen in the center of the divided scene. Using eq. (10) and eq. (11), the 2-D focusing is achieved. The diagram of improved CS algorithm is shown in Fig. 2.

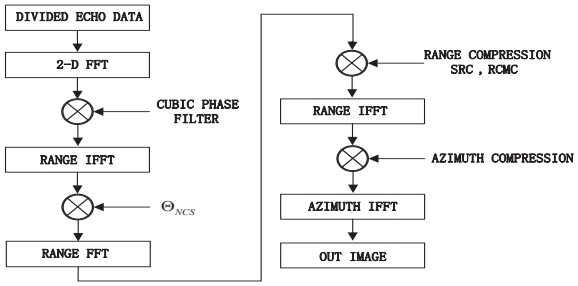

Fig. 2. The diagram of improved CS algorithm

4. SIMULATION RESULTS

The parameters of real SAR system were simulated to verify the feasibility and effectiveness of the algorithm presented in this paper. The center of scenario was selected at coordinate origin. The position of transmitter at time of coordinate origin at beam center crossing was (-441.13, -444.03, 630) km and the receiver was mounted at (-10, 3, 1) km. Simulation parameters were listed as TABLE Ⅰ.

TABLE Ⅰ Parameters

Parameters	Value
Carrier wavelength	0.04 m
Antenna size	9×5 m²
Velocity of transmitter	7300m/s
Squint angle	30°
Pulse-width	33us
Bandwidth	60 MHz
Sampling rate	72 MHz
PRF	2200 Hz

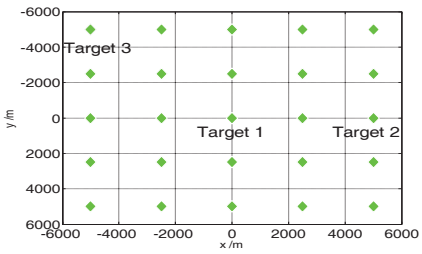

Fig. 3. Simulating targets in the scenario

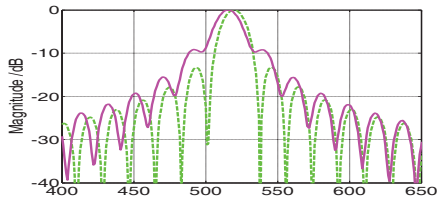

Fig. 4. Range profile of the spread function

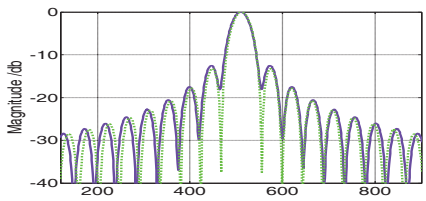

Fig. 5. Azimuth profile of the spread function

TABLE Ⅱ Imaging quality of different targets

	Performance	Target1	Target2	Target3
Range	PSLR(dB)	−13.26	−13.23	−13.23
	ISLR(dB)	−9.84	−9.86	−9.85
Azimuth	PSLR(dB)	−13.26	−13.26	−13.26
	ISLR(dB)	−10.10	−10.11	−10.09

Fig. 6. Imaging result

In Fig. 4, pink solid line is the range profile of the spread function of target 2 without NLCS, and green dotted line is the result with NLCS. It can be found that defocus has been overcome by using NLCS. Fig. 5 shows the azimuth profile of the spread function, where the purple solid line represents the result of target 3 with unified processing and the green dotted line is the result after sub-block processing. Obviously, using segmentation processing, defocusing in the azimuth direction can be overcome. Fig. 6 shows the scene imaging result, and the evaluation indexes of corresponding point targets are listed in TABLE Ⅱ.

5. CONCLUSION

An improved CS algorithm for one-stationary BiSAR squint mode is proposed in this paper. Signal model is firstly established, and after analyzing the characteristic of this kind of BiSAR, it can be found that the imaging algorithm is restricted by the space variability. Then improved CS algorithm is specifically described. The method of NLCS is introduced to deal with the space variability of equivalent range FM rate along the range direction, and the segmentation processing is introduced to overcome the space variability along the azimuth direction. Finally, the simulation is carried out to verify the feasibility and effectiveness of the algorithm presented in this paper.

6. REFERENCES

[1] Bai Xia, Sun Jinping and Mao Shiyi, “A novel approach for bistatic SAR imaging using a stationary receiver”, *Signal Processing, 2008*. ICSP 2008. 9th International Conference, pp. 2250 - 2253, 26 - 29 Oct. 2008.

[2] Xiaolan Qiu, Donghui Hu, and Chibiao Ding, “An Improved NLCS Algorithm With Capability Analysis for One-Stationary BiSAR”, Geoscience and Remote Sensing, IEEE Transactions on Volume 46, Issue 10, Part 2, pp. 3179 - 3186, Oct. 2008.

[3] Natroshvili, K., Loffeld, O., Nies, H., Ortiz, A.M. and Knedlik, S., “Focusing of General Bistatic SAR Configuration Data with 2-D Inverse Scaled FFT”, Geoscience and Remote Sensing, IEEE Transactions on Volume 44, Issue 10, Part 1, pp. 2718 – 2727, Oct. 2006.

[4] Loffeld, O., Nies, H., Peter, V. and Knedlik, S., “Models and Useful Relations for Bistatic SAR Processing”, Geoscience and Remote Sensing, IEEE Transactions on Volume 42, Issue 10, pp. 2031 – 2038, Oct. 2004.